

## THE X-RAY NOVA CENTAURUS X-4: COMPARISONS WITH A0620–00

JEFFREY E. McCLINTOCK<sup>1</sup>

Harvard-Smithsonian Center for Astrophysics

AND

RONALD A. REMILLARD<sup>1</sup>

Center for Space Research, Massachusetts Institute of Technology

Received 1989 April 3; accepted 1989 August 9

### ABSTRACT

Results are presented for the first simultaneous spectroscopic and photometric study of Cen X-4 in its quiescent state. The spectrum of this X-ray nova consists of a K5-K7V stellar part plus an accretion disk component. We confirm earlier determinations of the 0.629 day orbital period, and the  $\sim 150 \text{ km s}^{-1}$  K-velocity of the absorption lines; however, we find a system center-of-mass velocity of  $137 \pm 17 \text{ km s}^{-1}$ , which is substantially less than reported previously. We discuss and extend one of the models proposed by Chevalier *et al.* in which the secondary is a peculiar low-mass ( $\sim 0.1 M_{\odot}$ ) star viewed at a moderately low inclination angle ( $i \approx 35^{\circ}$ – $40^{\circ}$ ). Within the context of this model, our  $I$  and  $V-I$  light curves can be explained by the tidal distortion of the secondary plus some “excess light” from the splash point, the region where the accretion stream strikes the edge of the disk. Support for this interpretation is provided by the phase of the  $H\beta$  (emission-line) velocity curve. Cen X-4 is compared to the black-hole X-ray nova A0620–00. It is suggested that some differences may be due to the presence of a disk/star boundary layer in Cen X-4 and its absence in A0620–00.

*Subject headings:* stars: individual (Cen X-4, A0620–00) — X-rays: binaries

### I. INTRODUCTION

In most short-period ( $P \lesssim 1$  day) X-ray binaries the late-type secondary cannot be observed because the starlight is persistently overwhelmed by the emission from an X-ray heated accretion disk. About 10% of these systems, however, are X-ray novae, which hibernate for years or decades in a faint state ( $L_x \lesssim 10^{33} \text{ ergs s}^{-1}$ ;  $M_v \gtrsim 7$ ). A few such novae are nearby ( $d \sim 1$  kpc) and have relatively luminous K-type secondaries, which can be observed in quiescence. This is fortunate because the spectrum of the secondary provides important information about the orbital parameters, distance, and evolutionary state of the system. The two most favorable examples are the X-ray novae A0620–00 and Cen X-4. Earlier we reported on a study of A0620–00 in which we showed that the X-ray star is a probable black hole (McClintock and Remillard 1986). Here we present a similar study of Cen X-4, a neutron-star binary.

Cen X-4 was discovered during X-ray outburst in 1969 (Conner, Evans, and Belian 1969). During a second outburst in 1979 (Kaluzienski, Holt, and Swank 1980), it was identified optically with a star that had brightened by 6 mag to  $V = 13$  (Canizares, McClintock, and Grindlay 1980). About 3 weeks after the 1979 eruption a type I X-ray burst was observed, which indicates that the X-ray source is a neutron star (Matsuoka *et al.* 1980). Two weeks later the system had faded to  $V \approx 18$  and spectral observations by van Paradijs *et al.* (1980) showed that a late-type star (K3-K7) was present in the system.

Recently, two optical studies of Cen X-4 in quiescence have

appeared. The principal observational results are the following: Chevalier *et al.* (1989) discovered the orbital period,  $P_{\text{orb}} = 15.098 \text{ hr}$ , by collecting  $\sim 500$   $V$ -band photometric measurements over 4 yr. The persistent feature of their light curve is a double-humped modulation with a full amplitude of  $\approx 0.15 \text{ mag}$ ; however, the light curve also contains prominent, variable features that are difficult to explain.

Cowley *et al.* (1988) measured the absorption-line velocities of the K dwarf secondary and determined the value of the mass function to be  $0.23 M_{\odot}$ , in agreement with the value reported in this paper. The modest mass function further supports the argument for a neutron star primary (rather than a black hole). Cowley *et al.* also present some two-color ( $B$  and  $V$ ) photometric data; their light curve, which is much simpler than the yearly light curves of Chevalier *et al.*, resembles that of A0620–00 (McClintock and Remillard 1986).

The model favored by Cowley *et al.* invokes an evolved K-type secondary that fills its Roche lobe and has a radius about twice as large as the radius of a main-sequence K dwarf. For a plausible, assumed primary mass of  $1.4 M_{\odot}$  (e.g., see Pylyser and Savonije 1988), the system is viewed at an intermediate angle of inclination ( $i \approx 45^{\circ}$ ), and the light variations are attributed to the tidal distortion of the secondary.

Chevalier *et al.* (1989) challenge Cowley *et al.*'s interpretation of the data and reject their model for the secondary star. Chevalier *et al.* then present two widely different models: (1) a “classical scenario” in which the secondary is a peculiar low-density star (a stripped giant); the light curve is predominantly ellipsoidal, and the system is viewed at low inclination ( $i \sim 30^{\circ}$ ); and (2) a high-inclination ( $i > 80^{\circ}$ ) “alternative scenario” in which a main-sequence secondary fills only a small fraction of its Roche lobe volume; gas is transferred via a massive wind, and the complex light

<sup>1</sup> Visiting Astronomer at Cerro Tololo Interamerican Observatory, National Optical Astronomy Observatories, which is operated by the Association of Universities for Research in Astronomy, Inc., under contract with the National Science Foundation.

curve is attributed to the mutual eclipses of three components: the K star, an accretion disk, and an accretion wake, which is located near the neutron star.

In this paper we present the results of an optical study of the quiescent state. Our data are an important addition to earlier studies for two reasons: (1) We have made the first simultaneous spectroscopic and photometric observations, which is a crucial advantage because Cen X-4 in quiescence is highly variable. (2) Our *I*-band photometric data provide a cleaner measurement of the secondary (i.e., less adulterated by the blue disk spectrum) than earlier *B*- and *V*-band data. We present a single model (the “classical scenario” discussed by Chevalier *et al.*) that provides a consistent interpretation of our data, including our *V* and *I* light curves. However, some aspects of the light curves presented by Chevalier *et al.* remain unexplained.

## II. OBSERVATIONS

All of the data were taken at CTIO during 1987 April 24–28. On three nights, long-slit spectra were obtained with the 4 m telescope, R-C spectrograph, the Singer camera, and the photon-counting “2D-FRUTTI” detector. A typical observing sequence consisted of four consecutive 15 minute observations of Cen X-4 followed by a 5 minute observation of a K3 dwarf, HD 131719, which is located 4:5 from Cen X-4. A 2 minute He-Ne-A lamp spectrum was taken immediately before and after each individual observation. A flux calibration standard was observed each night. The total net observing time on Cen X-4 was  $\sim 13$  hr.

The 4130–6000 Å spectral range was sampled by 1530 data channels. The 2"2 slit yielded a spectral resolution of 4.1 Å (FWHM) when illuminated uniformly by the calibration lamp. On the first night (April 24 UT) only, there was a thin ice film on the entrance window of the detector. The ice reduced the throughput by up to 1.0 mag near the center of the passband; however, it did not affect the spectral resolution or the radial velocity determinations.

The wavelength stability of the spectrograph proved to be more than adequate: we determined the center of the He I  $\lambda 5015.7$  line in all (115) arc spectra and found that it did not shift more than 0.15 channels ( $\approx 12$  km s $^{-1}$ ) during any 15 minute observation; furthermore, the shifts were a smooth function of hour angle. Gross exceptions did occur on two nights at the same hour angle of  $\approx 2^{\text{h}}30^{\text{m}}$  west; the arc lines shifted by  $\sim 2$  channels and the corresponding object spectra were therefore discarded.

The data were wavelength-calibrated and binned in 1.24 Å intervals. An offset between the He-Ne-A lamp calibration and the “true” wavelength calibration was determined using two sources: (1) the central wavelengths of four night-sky lines were measured (prior to sky subtraction) in spectra of Cen X-4. (2) The wavelengths of seven, identifiable absorption features were measured for the K2 comparison star HD 131719. After these latter data were corrected for the velocity of the Earth and the radial velocity of HD 131719<sup>2</sup>, it was found that the night-sky lines and the absorption lines of HD 131719 are consistent with a single wavelength calibration. This implies that the neutral density filter required for observations of HD 131719 did not affect the wavelength calibration significantly. We then

<sup>2</sup> Heliocentric velocity of HD 131719 =  $16.6 \pm 0.1$  rms ( $N = 4$ ) with a zero point uncertainty of 0.5 km s $^{-1}$ ; measurements made on 1988 UT May 26, May 29, June 6, and July 3 (Latham 1988).

determined the center-of-mass velocities of the Cen X-4 absorption lines,  $V_0$ , and the H $\beta$  emission line,  $V\beta$ , which are discussed in § III. We estimate (conservatively) that the uncertainty in this calibration contributes  $\pm 15$  km s $^{-1}$  to the total error in  $V_0$  and  $V\beta$ .

We made photometric observations of Cen X-4 on four nights with the CF CCD instrument (RCA No. 5) on the 0.9 m telescope. A total of 60 *I*-band and 35 *V*-band exposures, each of 10 minute duration, were obtained. We extracted photometric measures for Cen X-4, five field stars, and four sky-background locations. In order to correct the photometric data for the effects of changing air mass and occasional cirrus clouds (on UT April 25 and April 27), we normalized the intensities of Cen X-4 and three reference stars by the intensities of the two brightest field stars. The light curves of the three remaining reference stars, which bracket the intensity of Cen X-4, provided an empirical measure of the rms uncertainty versus intensity, which we interpolated to obtain the following uncertainties ( $1 \sigma$ ) for an individual measurement of Cen X-4; 1.8% in *I* and 2.4% in *V*. Photometric standard stars were observed each night (Landolt 1983).

## III. RESULTS

### a) Absorption-Line Velocities

Sixteen spectra of Cen X-4 were formed (which have comparable statistical precision) by summing a few contiguous, 15 minute exposures. Sixteen corresponding velocity templates were created by summing the HD 131719 spectra that were recorded immediately before and after each Cen X-4 observing sequence. Three prominent emission features (H $\alpha$ , H $\beta$ , and He II  $\lambda 4686$ ) and the  $\lambda 5577$  night-sky line were excised from the spectra of Cen X-4 and replaced by the local mean count rate. The cross-correlation analysis was performed (Tonry and Davis 1979) over the full wavelength interval shortward of the NaD/He I feature (4130–5850 Å). The central velocities of the cross-correlation peaks, which were determined using a parabolic fit, are listed in Table 1 and plotted in Figure 1a. The velocity data are well fitted by a simple sinusoid ( $\chi^2_r = 1.1$ ) with the orbital period fixed at the photometric period; the dynamical results are summarized in Table 2A. We note that

TABLE 1  
HELIOCENTRIC RADIAL VELOCITIES FOR CEN X-4

HJD 2,440,000 +	Spectroscopic Phase	Absorption-Line Velocity (km s $^{-1}$ )	H $\beta$ Emission-Line Velocity (km s $^{-1}$ )
6909.5741.....	0.995	286 $\pm$ 29	128 $\pm$ 45
6909.6431.....	0.105	271 $\pm$ 47	186 $\pm$ 45
6909.7068.....	0.206	129 $\pm$ 35	37 $\pm$ 60
6909.7707.....	0.308	127 $\pm$ 40	62 $\pm$ 45
6909.8368.....	0.413	–39 $\pm$ 38	79 $\pm$ 55
6910.5606.....	0.564	–8 $\pm$ 36	141 $\pm$ 60
6910.5919.....	0.613	54 $\pm$ 29	153 $\pm$ 45
6910.6444.....	0.697	87 $\pm$ 30	253 $\pm$ 40
6910.7162.....	0.811	151 $\pm$ 38	250 $\pm$ 55
6910.7442.....	0.855	256 $\pm$ 22	252 $\pm$ 40
6910.7884.....	0.926	...	199 $\pm$ 55
6912.5546.....	0.733	112 $\pm$ 24	152 $\pm$ 35
6912.6958.....	0.958	242 $\pm$ 23	178 $\pm$ 35
6912.7215.....	0.998	294 $\pm$ 24	178 $\pm$ 40
6912.7795.....	0.091	299 $\pm$ 34	139 $\pm$ 40
6912.8552.....	0.211	136 $\pm$ 30	138 $\pm$ 40
6912.8819.....	0.253	172 $\pm$ 27	182 $\pm$ 50

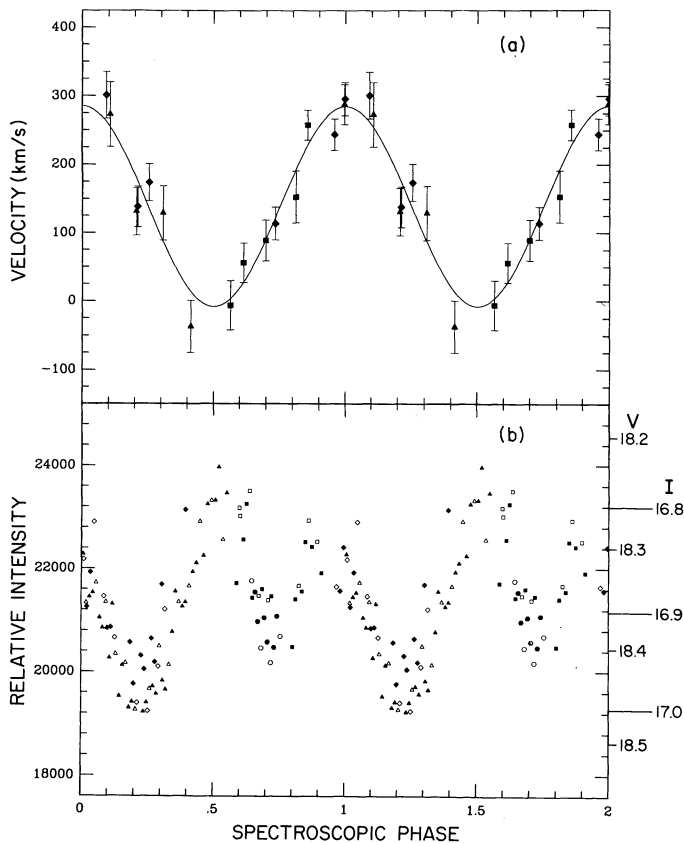


FIG. 1.—Simultaneous spectroscopic and photometric data for Cen X-4 obtained at CTIO in 1987 April. The different symbol shapes correspond to different observing nights: the triangles, squares, diamonds, and hexagons correspond respectively to UT April 24, 25, 27 and 28. (a) Heliocentric radial velocities of the K-dwarf secondary. The smooth curve is a fit to a circular orbit model (Table 2A). (b) Folded CCD light curve composed of 95 individual measurements. The solid symbols are  $I$  band data and the open symbols are  $V$  band data, which have been scaled to match the mean intensity in the  $I$  band. The uncertainty for an individual  $I$ -band measurement is  $\sim 0.02$  mag (§ II). For the  $V$  magnitudes inferred from the  $I$  band data there is a small additional uncertainty ( $\approx 0.03$  mag) due to orbital color changes (Fig. 7b).

our results are in good agreement with Cowley *et al.* (1988) except for the value of the systemic velocity. We find  $V_0 = 137 \pm 17$  km s $^{-1}$ , whereas Cowley *et al.* report a much larger value,  $V_0 = 234 \pm 8$  km s $^{-1}$ .

#### b) Light Curves

All of the individual CCD measurements of Cen X-4 are displayed in the folded light curve in Figure 1b. The intensity is seen to vary smoothly by as much as 17%. The light curve exhibits the (15.1 hr) periodic, double-humped structure observed by Chevalier *et al.* (1989) and Cowley *et al.* (1988)—behavior typical of Cen X-4 in its quiescent state,  $V_{ave} \lesssim 18.3$ .

Our two brightest field stars (see § II) are the same two “comparison stars” used by Chevalier *et al.* (1989). Our  $V$  magnitudes agree with theirs to within 0.04 mag, which facilitates a direct comparison between the present study and their 4 yr photometric study of Cen X-4. Our  $I$  magnitude for the two stars are 15.75 and 15.99 ( $\pm 0.04$  mag), where the star that is brighter in  $I$  is also brighter in  $V$ .

The orbital period of Cen X-4 given by Chevalier *et al.* (1989) is  $0.629063 \pm 0.000021$  days. This period does not allow us to

TABLE 2

ORBITAL PARAMETERS FOR CEN X-4<sup>a</sup>

Parameters	Values
A. Absorption Lines <sup>b</sup>	
$V_0$ (km s $^{-1}$ )	$137 \pm 17^c$
$K$ (km s $^{-1}$ )	$146 \pm 12$
$T_0$ (HJD 2,440,000+)	$6909.5771 \pm 0.0073$
$a_c \sin i$ ( $R_\odot$ )	$1.82 \pm 0.15$
$f$ ( $M/M_\odot$ )	$0.20 \pm 0.05$
B. H $\beta$ Emission Line <sup>b</sup>	
$V\beta$ (km s $^{-1}$ )	$154 \pm 19^c$
$K\beta$ (km s $^{-1}$ )	$58 \pm 16$
$T\beta^d$ (HJD 2,440,000+)	$6909.468 \pm 0.029$
C. Photometric Data	
$P$ (d)	$0.629063 \pm 0.000005$
$T_{phot}^e$ (HJD 2,440,000+)	$6909.756 \pm 0.008$

<sup>a</sup> Uncertainties are  $1\sigma$  confidence limits; times and velocities are heliocentric.

<sup>b</sup> Circular orbit solution with the orbital period fixed at 0.629063 days.

<sup>c</sup> Error dominated by the uncertainty in the velocity zero point,  $\pm 15$  km s $^{-1}$  (§ II), which has been added in quadrature to the statistical error from the fit.

<sup>d</sup> Time of maximum H $\beta$  velocity; corresponds to spectroscopic phase  $0.85 \pm 0.05$ .

<sup>e</sup> Time of primary (deeper) minimum; occurs  $0.022 \pm 0.011$  days after spectroscopic phase 0.25.

match their deep minimum (which occurs at their photometric phase zero) with ours; however, it does give a precise match between their deep minimum and our shallow minimum. The same mismatch was found by Chevalier *et al.* when they computed the phase of their light curve relative to the light curve of Cowley *et al.* (i.e., Chevalier *et al.*'s deep minimum corresponds in phase to Cowley *et al.*'s shallow minimum). This discrepancy is quite surprising because the distinctive, asymmetric shape of our light curve resembles so closely the shape observed by Chevalier *et al.*, particularly in 1986 May (see their Fig. 2): both light curves cross a similar range of  $V$  mag; for both, the shallow minimum follows the higher maximum, and the relative phase between these features is significantly less than a fourth of a cycle. The 1985 March profile observed by Chevalier *et al.* is similar in shape, although the average intensity is depressed by  $\sim 0.15$  mag.

We have attempted to isolate the light curve profiles obtained by Chevalier *et al.* that most closely resemble our light curve in order to determine whether an alternative period can better reconcile all of the photometric data. Our efforts to match our deep minimum with those observed by Chevalier *et al.* in 1986 May (527–530 cycles) and 1985 March (1204–1207 cycles) proved unsuccessful. We are therefore forced to conclude that our deep minimum corresponds to Chevalier *et al.*'s shallow minimum. Combining our data with theirs in this manner determines a refined photometric period of  $0.629063 \pm 0.000005$  days, which disagrees somewhat ( $2.5\sigma$ ) with the “revised” spectroscopic period found by Cowley *et al.* (1988). In § IVd–IVe we discuss further the peculiarities of the light curve.

#### c) Emission-Line Data

We examined the Balmer lines in 17 spectra; the observation times are listed in Table 1. The line profiles typically appear



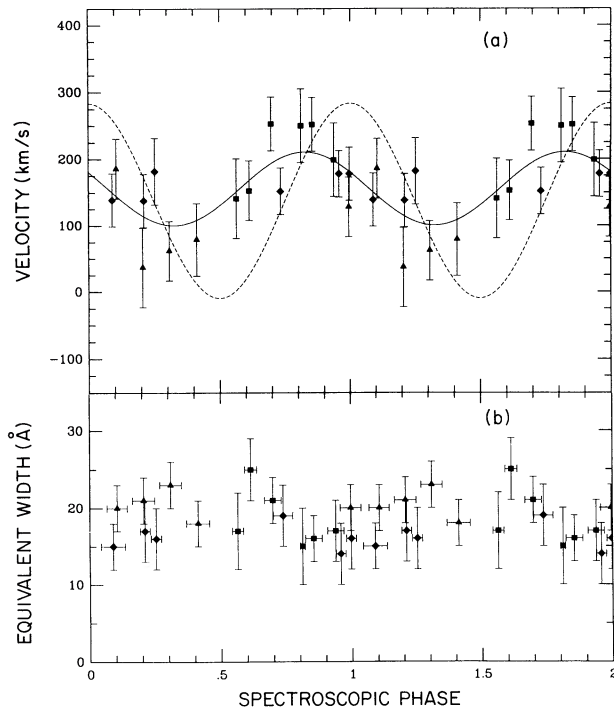


FIG. 2.— $H\beta$  emission-line data for Cen X-4. The symbols have the same meaning as in Fig. 1. (a) Heliocentric radial velocities of the Balmer emission-line region. The solid curve is a circular-orbit fit to the data (Table 2B). For comparison, the fit to the absorption-line data is also shown (dashed curve). (b) Equivalent width of  $H\beta$  versus orbital phase. The horizontal error bars, which apply also to the data points plotted in Figs. 1a and 2a, correspond to the start and end times of data acquisition.

asymmetric and the continuum level is often poorly defined. We therefore investigated several techniques for determining radial velocities and equivalent widths, all of which gave similar results.

The velocities determined for  $H\beta$  are plotted in Figure 2a and listed in Table 1. (The  $H\gamma$  velocities are poorly determined and are not presented.) The data can be fitted by a sinusoid ( $\chi^2_v = 1.0$ ) with the dynamical parameters that are given in Table 2B. The apparent center-of-mass velocity is consistent with the absorption-line value (Table 2A), in contrast to the puzzling difference of  $\sim 130 \text{ km s}^{-1}$  found by Cowley *et al.* (1988). The velocity amplitude of  $H\beta$ , which is comparable to the values reported by Cowley *et al.*, is about a third as large as the absorption line amplitude.

The most interesting result is the phase lag of the absorption-line velocities relative to the  $H\beta$  velocities: the maximum  $H\beta$  velocity occurs at absorption-line phase  $0.85 \pm 0.05$  (Fig. 2a). Cowley *et al.* have reported very similar results on two occasions when Cen X-4 was comparably bright, and an even smaller phase difference was obtained on a third occasion when Cen X-4 was exceptionally faint. Therefore, the near-agreement in phase between the absorption-line and emission-line velocities is a persistent feature of Cen X-4.

The equivalent width of the  $H\beta$  line is plotted in Figure 2b. No significant variations are present at the orbital period. In particular, there is no evidence for an eclipse of the line-emission region.

#### d) Spectral Class of the Secondary

We used the sine-wave fit to the velocity data (Table 2A) to Doppler-correct the individual spectra to the approximate rest frame of the secondary. The grand sum of the 16 velocity-shifted spectra and the spectra of two comparison stars is shown in Figure 3.

We have classified the spectrum of the secondary as a K5-7 dwarf as follows (Abt *et al.* 1968; Keenan and McNeil 1976; Jacoby, Hunter, and Christian 1984; Figs. 3 and 5 in McClintock and Remillard 1986): the continuum contains a  $\sim 200 \text{ \AA}$  wide depression due to  $\text{MgH}$  ( $\lambda 5180$ ) and the  $\text{TiO}$  band at  $\lambda\lambda 5200\text{--}4954$ , which is a hallmark of a K dwarf. The strength of the  $\text{Ca I } \lambda 4226$  line, the  $\text{NaD}$  doublet and the  $\text{MgH } \lambda 4780$  feature establish that the Cen X-4 secondary is approximately luminosity class V.

The strengths of several metallic lines (e.g.,  $\text{Fe I } \lambda 4383$ ), with due allowance for a continuum disk component, rule out a spectral type as late as M0. Similarly, the strong  $G$  band,  $\text{Ca I } \lambda 4226$  line and other features rule against a spectral type as early as K3. Overall the metallic lines indicate that the spectral type is near K5. The presence of a modest  $\text{MgH } \lambda 4780$  feature, however, suggests a somewhat later spectral type, about K7. We therefore conclude that the spectral class of the secondary is K5-7V. Chevalier *et al.* (1989) reached the same conclusion (K7V) using a different approach and a lower resolution spectrum of photometric quality.

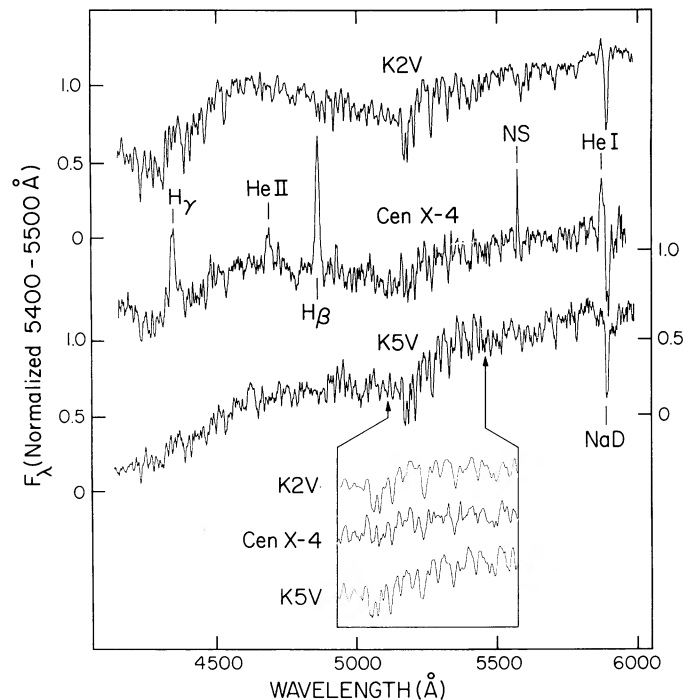


FIG. 3.—Grand-sum spectrum of Cen X-4 ( $T_{\text{obs}} = 13.2 \text{ hr}$ ) in the rest frame of the K-dwarf secondary (see text), and the spectra of two comparison stars. The spectra are not of high photometric quality and the overall continuum shapes may be somewhat misleading. The fluxes have been normalized arbitrarily to unity at  $5450 \text{ \AA}$ ; the flux scales on the left apply to the comparison stars and the scale on the right to Cen X-4. The feature marked “NS” is an artifact due to a night-sky emission line. The inset blowup shows the metallic absorption lines in more detail in the interval  $5100\text{--}5450 \text{ \AA}$ . The spectral resolution is  $\sim 5 \text{ \AA}$  (FWHM).

## IV. DISCUSSION

We favor one of the models for Cen X-4 proposed by Chevalier *et al.* (1989), which is consistent with all of our observational results. Before discussing this model we discard two alternative models for the secondary.

## a) Two Unlikely Models for Cen X-4

A main-sequence K-dwarf secondary would fill only  $\sim 10\%$  of the volume of its Roche lobe, thereby making it difficult to account for mass transfer and the amplitude of the light curve (Chevalier *et al.* 1989; Cowley *et al.* 1988). Nevertheless, Chevalier *et al.* attempt to rescue this model in order to explain the variable and asymmetric features in their *V*-band light curve (particularly the troublesome dip which is sometimes present at spectroscopic phase 0.33). They posit that Cen X-4 is viewed nearly edge on ( $i > 80^\circ$ ) and that the K dwarf feeds its primary via a stellar wind.

Although this model can account for the irregularities in their light curve, we feel that it is untenable for several reasons, including the following: (1) The model invokes mass transfer via a wind with an isotropic mass-loss rate from the secondary of  $10^{-9}$ – $10^{-8} M_\odot \text{ yr}^{-1}$  (or possibly a magnetic “funneling” of a lesser wind); there is no evidence whatsoever that even a rapidly rotating K dwarf could drive such a massive wind. (2) The high inclination ( $i > 80^\circ$ ) required to explain the peculiarities in the light curve implies that the compact X-ray source will be eclipsed by the secondary. The eclipse may have been missed during the 1979 outburst because of the scanty observations by the *Ariel V* and *Hakucho* satellites (as argued by Chevalier *et al.*); however, during the 1969 apparition, the *Vela* satellites would have detected an eclipse—Cen X-4 was observed each minute for hours at a time on many occasions—and no eclipse was seen (Evans, Belian, and Conner 1973; Belian, Conner, and Evans 1972, and references therein). (3) The optical light curve is attributed to the eclipse of different components—the K star, the accretion disk, and a wake of accreted matter near the primary. The differing temperatures of these components might be expected to produce much larger orbital color changes than are observed (Fig. 7b; Fig. 6 in Cowley *et al.* 1988). (4) The value of the mass function (for  $i \approx 90^\circ$ ) dictates a primary mass of  $\lesssim 1.0 M_\odot$  ( $2\sigma$  for  $M_c \lesssim 0.9 M_\odot$ ); on evolutionary grounds it seems improbable that Cen X-4 contains such a low-mass neutron star (e.g., Pylyser and Savonije 1988). Thus, this model solves the problem of the variable light curve, but in doing so it creates far greater problems, and so we reject it.

An evolved K-star secondary, which fills its Roche lobe, must be more massive than  $0.8 M_\odot$  or it would not have left the main sequence in a Hubble time. The radius of its Roche lobe is therefore greater than  $1.3 R_\odot$ , which implies a distance of at least 2.5 kpc (see below). This model, which is favored by Cowley *et al.* (1988), appears to us and to Chevalier *et al.* (1989) to be untenable because the observed type I X-ray bursts, which were of unprecedented intensity ( $I_{\text{max}} \approx 25$  Crab), would then have grossly exceeded the Eddington luminosity (see below). A second counterargument is the observed low rate of mass transfer. The  $3 \times 10^{43}$  ergs radiated during the 1979 outburst (Kaluzienski, Holt, and Swank 1980) implies a decade-average accretion flow of  $\sim 2 \times 10^{-11} M_\odot \text{ yr}^{-1}$ , which is at least an order of magnitude less than is expected if the transfer is driven by the evolution of a secondary that has recently left the main sequence (Webbink, Rappaport, and Savonije 1983). Therefore, we also reject this model.

## b) A Preferred Model

The model we favor (Chevalier *et al.* 1989; their “classical scenario: case C”) is motivated, in part, by the following two considerations (1) During quiescence, the residual X-ray flux (van Paradijs *et al.* 1987) and the optical disk emission attest to the ongoing transfer of mass and argue strongly that the secondary fills its Roche lobe. (2) The average density of a star that fills its Roche lobe is determined solely by the orbital period,  $\rho = 110/P^2$  (hours), a result that follows by combining Kepler’s Law with Paczyński’s (1971) formula for the Roche lobe radius. Thus, the density of the secondary is  $0.5 \text{ g cm}^{-3}$ , which is only 10% of the density of a main-sequence K5–7 star ( $\rho = 4.7 \text{ g cm}^{-3}$ ; Popper 1980).

The above conclusion implies that the secondary is a peculiar star; consequently its distance cannot be inferred directly from its spectral type. Fortunately, upper and lower bounds on the distance are provided by the detection of the two brightest type I X-ray bursts ever observed ( $I_{\text{max}} \approx 25$  Crab), if one assumes that the peak flux corresponds to the Eddington luminosity of a  $\sim 1.4 M_\odot$  neutron star. For a discussion of the uncertainties see Chevalier *et al.* (1989) who conclude that the distance to Cen X-4 is very probably  $d = 1.2 \pm 0.2$  kpc. We have re-examined the arguments and the data and concur; however, we consider a broader range of distance,  $0.7 \text{ kpc} < d < 1.9 \text{ kpc}$  (see Fig. 4), within which Cen X-4 is almost certain to lie.

The mean apparent magnitude of the optical counterpart is  $V \approx 18.35$  (Fig. 1). When Chevalier *et al.* (1989) observed Cen X-4 at the same average brightness, they found that the disk contributed  $\sim 25$ – $30\%$  of the *V*-band flux. Our higher resolution spectra support their finding in an independent way: the Cen X-4 absorption lines are somewhat shallow (Fig. 3), which implies that they are diluted by a modest ( $\sim 0.2$ – $0.4$  mag) continuum component. Thus, the mean magnitude of the K star is  $\sim 18.7$  and its dereddened magnitude is 18.4 (Blair *et al.* 1984), with an estimated uncertainty of 0.2 mag, which we disregard as negligible compared to the distance uncertainties discussed above. The K star’s absolute magnitude is therefore in the range  $M_V = 8.0 \pm 1.0$  (Fig. 4a).

The star’s radius depends only on its absolute magnitude and effective temperature ( $T_e = 4000$ – $4300$  K), which is fixed by its K5–7 spectral type and the distance (Popper 1980). Consequently, as shown in Figure 4b, the allowed range of radius is  $0.3 R_\odot < R_c < 1.1 R_\odot$ , and the most likely value is  $\sim 0.6 R_\odot$ . The star’s radius determines its mass, since its mean density is fixed at  $0.5 \text{ g cm}^{-3}$  (see above). The allowed range of mass is  $0.01 \leq M_c \leq 0.44$ , and the most probable value is  $\sim 0.1 M_\odot$  (Fig. 4c).

We now use the mass function  $(M_x \sin i)^3 / (M_x + M_c)^2 = 0.20 \pm 0.05 M_\odot$  to determine the orbital inclination. The mass of the neutron star,  $M_x$ , is at least a Chandrasekhar Mass, and a long history of accretion has probably added an additional fraction of a solar mass (e.g., Pylyser and Savonije 1988). We have therefore computed the inclination for two values of  $M_x$  over the full allowed range of the K star’s mass; the results are shown in Figure 5. The plane of the orbit is fairly close to the plane of the sky: the most likely value of the inclination angle is  $i \approx 30^\circ$ – $35^\circ$ , and the extreme range is  $26^\circ < i < 44^\circ$ .

c) The Phase of the H $\beta$  Velocity Curve

We (and Cowley *et al.* 1988) have measured only the center of gravity of a broad Balmer profile, which is probably composed of multiple components (e.g., Horne and Marsh

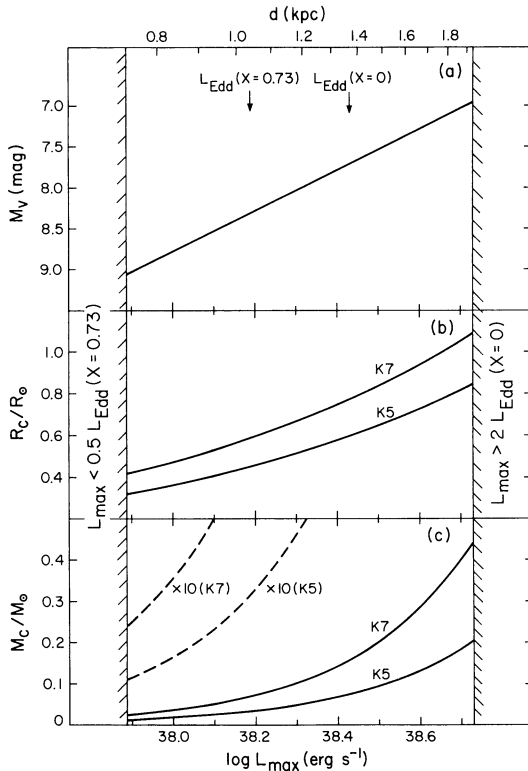


FIG. 4.—The most probable distance to Cen X-4 is  $d = 1.2$  kpc, which corresponds to a peak burst luminosity at the Eddington limit; it is very probable that  $0.7$  kpc  $< d < 1.9$  kpc, as indicated by the vertical hatched lines. If so, the absolute magnitude, size, and mass of the Roche-lobe filling secondary are constrained to the ranges of values shown here, as described in the text. The pairs of curves in (b) and (c) show the sensitivity to spectral type. The dashed curves in (c) are replots of the corresponding solid curves with the ordinate values multiplied by 10.

1986). Consider, nevertheless, the following tentative interpretation of the  $H\beta$  velocity curve. The line profile very probably contains a broad component from the entire disk; its amplitude is expected to be small ( $K M_c / M_x \sim 10$  km s $^{-1}$ ), and we ignore it. A second component of the  $H\beta$  line may arise from a splash region (bright spot) on the outer disk, or from the impinging accretion stream near the splash region. Such a component is responsible in cataclysmic variables for the so-called S-wave velocity curve. The velocity of this component will be (approximately) Keplerian and therefore large (roughly few hundred km s $^{-1}$ ).

In the case of Cen X-4, if the  $H\beta$  line is dominated by these two emission components, then the phase of the  $H\beta$  curve ( $\phi = 0.85$ ) is determined solely by the  $H\beta$  emission from the splash region. (We assume that the disk emission is cylindrically symmetric.) In this picture, the phase of the  $H\beta$  velocity curve determines the azimuthal location of the splash point—it is  $\sim 50^\circ$  ahead of the secondary, as illustrated in Figure 6. On the other hand, the interpretation of the amplitude of the  $H\beta$  velocity curve (58 km s $^{-1}$ ) is too uncertain to provide a useful constraint on the model.

The above interpretation of the  $H\beta$  phase is not unique; there are other possible locations for emitting gas in accreting binary systems (e.g., Cowley *et al.* 1988; Gilliland and Kemper 1980). Nevertheless, we find it attractive to locate the source of the velocity-variable component of  $H\beta$  at the splash point because this ties in with the interpretation of our light curve that is given in the following subsection.

d) The Light Curve: Ellipsoidal Variations

In our model, the inclination is too low for eclipses to play a role in shaping the light curve. Qualitatively the appearance of the light curve suggests ellipsoidal variability<sup>3</sup>: there are two

<sup>3</sup> "Ellipsoidal" is a misnomer that we have retained for historical reasons. Russell (1945) and others derived the light curves of tidally distorted stars, which underfilled their Roche lobes, by approximating their shapes as triaxial ellipsoids. For the filled-lobe model described here, we have, of course, used the exact Roche geometry. It is assumed here and elsewhere that the secondary's rotation is phase-locked to the orbital motion (Zahn 1977).

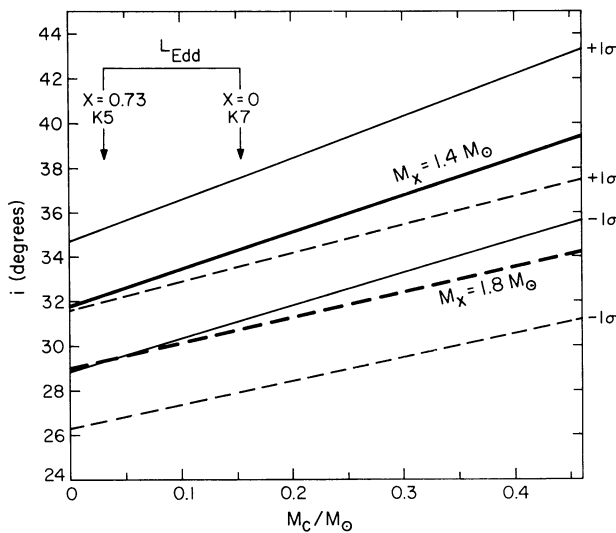


FIG. 5.—The orbital inclination angle vs. the allowed values of the mass of the companion (see Fig. 4c) for two possible masses of the neutron star primary. The heavy solid and heavy dashed lines were computed using the value of the mass function, and the lines marked  $\pm 1 \sigma$  correspond to one standard deviation away from the best value of the mass function (Table 2A).

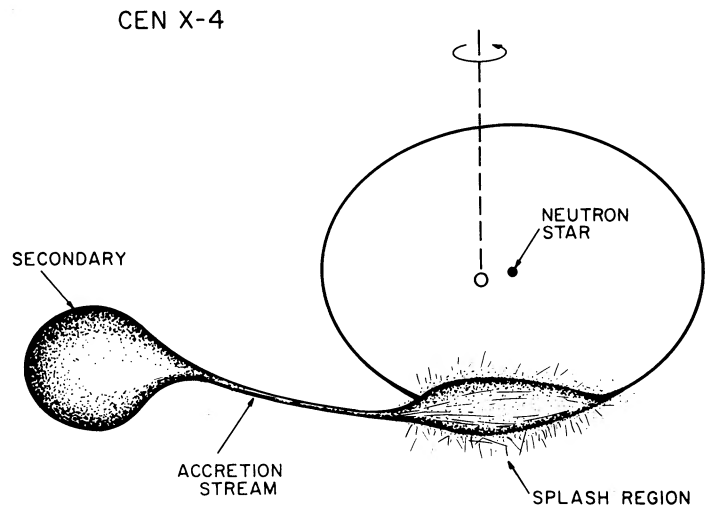


FIG. 6.—Schematic sketch (to approximate scale for  $i = 40^\circ$ ) for the model discussed in the text. The system center of mass is marked by the small open circle. The view is at spectroscopic phase 0.6; the splash region on the edge of the accretion disk is in clear view and its contribution to the light is a maximum. A quarter of an orbital cycle later ( $\phi = 0.85$ ) the splash region will be receding at maximum velocity and the  $H\beta$  radial velocity will reach a peak.



maxima and two minima per orbital cycle, and for 4 years the minima have occurred near spectroscopic phases 0.25 and 0.75. Quantitatively the ellipsoidal model can account for most of the observed modulation. Using a program written by Yoram Avni (1978), we computed models of the secondary for the observed K5-7V spectral type ( $T_e = 4000\text{--}4300$  K and  $\log g \approx 4.0$ ). The limb darkening coefficients for the  $V$  band (5500 Å) and the  $I$  band (9000 Å) were taken to be 0.88 and 0.56, respectively (Al-Naimiy 1978). The appropriate gravity darkening for a convective envelope (Lucy 1967) was computed using the Planck function. We assume that the secondary fills its Roche lobe (§ IVb); consequently the only remaining parameters are the orbital inclination angle ( $i$ ) and the mass ratio ( $q \equiv M_x/M_c$ ).

The folded  $V$  and  $V-I$  light curves are shown in Figure 7. An ellipsoidal model cannot account for the unequal maxima because it predicts maxima with precisely equal amplitude. Furthermore, it cannot account for the very different depths of the minima for plausible, moderate-inclination models of Cen X-4 (see Bochkarev, Karitskaya, and Shakura 1979). The azimuthally symmetric portion of the accretion disk is known to be an important second (unmodulated) source of light (§ IVb). Here we invoke a third source of light—a local structure on the outer disk—to account for the unequal maxima and minima in the light curve. In the following we will show that the azimuthal position of this light source on the

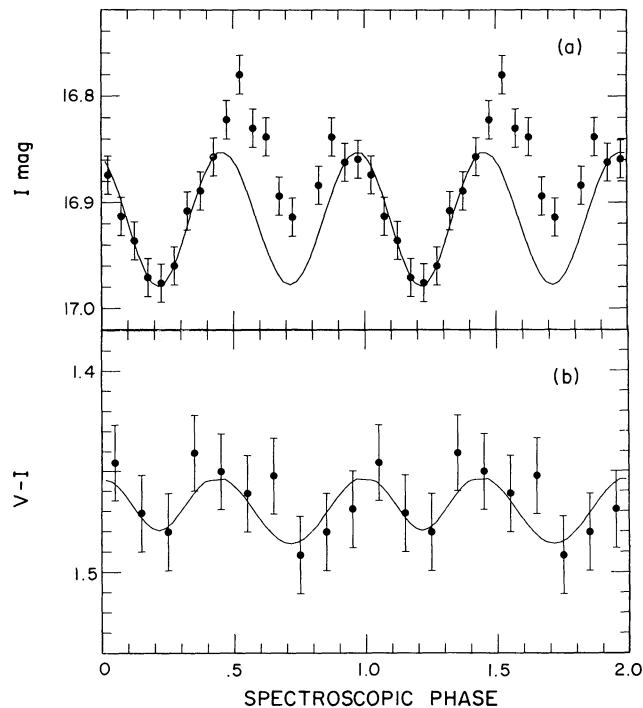


FIG. 7.—Folded  $V$  and  $V-I$  light curves, which are a different representation of the same data plotted in Fig. 1b. The solid curves are a fit to an ellipsoidal model (see text). The phase of the model is determined by the phase of the primary photometric minimum, which occurs slightly later than the time of zero velocity (see Table 2C). (a)  $I$  band data binned in 20 equal intervals of orbital phase. There are typically two or three independent measurements per phase bin. The error bar is the 1.8% uncertainty for a single measurement that is described in § II. (b)  $V-I$  color data binned in 10 intervals of phase. The  $V$  mag at the time of an  $I$ -band measurement was determined by interpolating the adjacent  $V$ -band measurements.

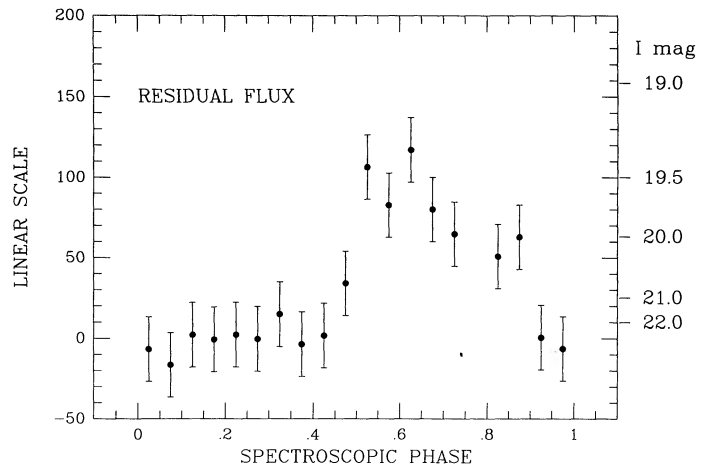


FIG. 8.—The difference in Fig. 7a between the  $I$ -band data and the ellipsoidal model. The residual flux near phase 0.6 is  $\sim 10\%$  of the total (cf. Fig. 7a); it is attributed to a bright region on the disk, which is produced by the impact of the accretion stream (see Fig. 6).

outer disk agrees with the position of the  $H\beta$  source discussed above (see Fig. 6).

To begin, we seek an ellipsoidal model that matches the deeper minimum and the lesser maximum. The best fit to the  $I$  light curve is obtained for  $i = 38^\circ$  and  $q \sim 15$ , with strong dependence on  $i$  ( $\pm 1^\circ$ ) and weak dependence on  $q$  ( $3 \lesssim q \lesssim 30$ ); the model fit is shown in Figure 7a.<sup>4</sup> The  $V-I$  color variations (Fig. 7b) support this model: a double-sine wave fitted to the data gives a full amplitude of  $0.017 \pm 0.006$  mag, which closely matches the predictions of the model for  $i = 38^\circ$  and  $q \sim 15$ , as shown in Figure 7b.

Further support for the model is provided by the phase dependence on  $i$  ( $\pm 1^\circ$ ) and weak dependence on  $q$  ( $3 \lesssim q \lesssim 30$ ) intensity occurs at spectroscopic phase 0.6, when one expects a nearly frontal view of the splash region, based on studies of cataclysmic variables (e.g., Robinson 1976). Furthermore, the maximum velocity amplitude of the  $H\beta$  source occurs one fourth phase later ( $\phi = 0.85 \pm 0.05$ ). Thus, our model provides a self-consistent interpretation of the “excess light” and the velocity-variable  $H\beta$  emission by ascribing both of them to the splash region.

#### e) The Light Curve: Secular Variability

As indicated above, we believe that an ellipsoidal model accounts for the dominant and stable features in the light curve. There remains, however, the vexing secular variability observed by Chevalier *et al.* (1989), which cannot be explained readily by emission from the splash region. This variability is most prominent near the minimum at spectroscopic phase 0.25 (photometric phase 0.5 in their Fig. 3). Chevalier *et al.* find that the amplitude and profile of this minimum are erratic, and that a second dip (centered at spectroscopic phase 0.33) sometimes develops. On the other hand, this same minimum observed by Cowley *et al.* (phase zero in their Fig. 5) and ourselves (Fig. 1b

<sup>4</sup> The model does not include a DC light contribution from the accretion disk because the existing data do not permit a deconvolution of the disk and K-star fluxes. However, the effects of the DC light appear to be small. For  $I_{\text{DISK}} = 18.8$  and  $(V-I)_{\text{DISK}} = 0.9$  (obtained by extrapolating the disk spectrum in Fig. 6b in Chevalier *et al.* 1989), the amplitude of the model curve would decrease by only  $\approx 0.01$  mag, and the orbital inclination would increase only slightly from  $38^\circ$  to  $40^\circ$ .

and Fig. 7a) is deep and relatively symmetric, similar to the primary minimum we observed for A0620-00 (McClintock and Remillard 1986).

To attempt to accommodate the observations of Chevalier *et al.* (1989) using our model, we must move the splash region by  $\sim 0.5$  in phase so that the excess light peaks near spectroscopic phase 0.25. The splash region would then be diametrically opposite the K star, which would appear to be a very unpromising location. It should be possible to test this idea by making further simultaneous photometric and  $H\beta$  velocity measurements. In any case, we believe that new data are required to explain the light curve anomalies observed by Chevalier *et al.* Two additional mechanisms that might produce the anomalies and deserve consideration are star spots and X-ray/UV heating.

Star spots are well-known features on late-type stars that have rotational speeds comparable to Cen X-4's secondary,  $V \sin i \approx 60 \text{ km s}^{-1}$ . Large, dark spots commonly produce  $\sim 0.2$  mag rotational light curves that vary in shape and amplitude on the desired time scale of months to years (e.g., Vogt 1975; Bouvier and Bertout 1988). Two examples with spectral types comparable to Cen X-4 are the K4 star V410 Tau (Vrba, Herbst, and Booth 1988) and the Pleiades K dwarf HII 1883 (Stauffer, Dorren, and Africano 1986).

X-ray heating was considered by Chevalier *et al.* (1989); they conclude that heating of the K star by the *observed* X-ray source (for an assumed thermal bremsstrahlung spectrum with  $kT = 1-5 \text{ keV}$ ) would contribute a negligible fraction ( $\sim 1\%$ ) of the  $V$ -band light. As they point out, however, there may be a hard X-ray component ( $kT > 5 \text{ keV}$ ) that produces sizable heating effects and that nevertheless could have escaped detection. Similarly, a very soft component ( $kT \lesssim 0.1 \text{ keV}$ ) might produce significant heating and also could have gone undetected. An attractive feature of this ad hoc model is that the major irregularities occur near spectroscopic phase 0.25, precisely where X-ray/UV heating effects are expected to occur. A heating model predicts significant color changes; unfortunately Chevalier *et al.* (who obtained "comparative exposures" in the  $U$ ,  $B$ , and  $I$  passbands) do not present multicolor data. We note that the quiescent system gets somewhat bluer as it brightens from  $V \approx 18.5$  to 18.3 (Fig. 7 in Cowley *et al.*) and that it gets much bluer and the light curve becomes erratic as the system brightens to  $V \lesssim 18$  (Fig. 2 in Chevalier *et al.*), which suggests that heating of the K star may be important.

#### f) Comparison with A0620-00

If we set aside the dynamical data for a moment, Cen X-4 and A0620-00 (McClintock and Remillard 1986) appear to be strikingly similar. Their optical counterparts have about the same absolute (and apparent) magnitudes and spectral characteristics, both at outburst maximum and during quiescence. In particular, the secondaries in both systems are approximately spectral class K5V. The quiescent light curves, which are primarily due to the tidal distortion of the secondaries, have the same "double-humped" shape and about the same amplitude. The peak X-ray luminosities during outburst and the average mass transfer rates (§ IVa; McClintock *et al.* 1983) are very nearly the same.

It is the dynamical data that expose the differences. Of first importance is the mass function. A0620-00's large mass function ( $3.2 M_{\odot}$ ) argues that the primary is a black hole, whereas the mass function and X-ray burst data show that Cen

X-4 contains a neutron star. The orbital period itself points up a difference between the secondaries: a Roche-lobe filling secondary in A0620-00 ( $P_{\text{orb}} = 7.8 \text{ hr}$ ) is 3.8 times as dense as the secondary in Cen X-4 (see § IVb). Finally, the large systematic velocity of Cen X-4 ( $137 \pm 17 \text{ km s}^{-1}$ ) indicates that it is a halo-population object, whereas A0620-00's velocity ( $-5 \pm 12 \text{ km s}^{-1}$ ) suggests that it may be a Population I object. For a discussion of evolutionary scenarios for Cen X-4 and A0620-00 see Pylyser and Savonije (1988) and references therein.

We now ask, what are other differences between Cen X-4 and A0620-00 that may be linked to the differences between a neutron-star accretor and a black-hole accretor? Consider first the outburst state. We are aware of no distinctions based on optical or UV data. In the X-ray band, however, there are at least two important distinctions. Cen X-4 displayed a typical thermal X-ray spectrum with  $kT = 5 \text{ keV}$ , whereas A0620-00 had a remarkably "soft" spectrum with  $kT = 1 \text{ keV}$ . A soft spectrum appears to be a fairly reliable, but not an infallible (e.g., Cir X-1) signature of a black hole (White and Marshall 1984); sources of soft photons, which may be peculiar to black holes, have been suggested by White, Fabian, and Mushotzky (1984) and Kazanas (1986). The occurrence of type I X-ray bursts is a second difference; bursts, which are neutron-star shell flashes, were observed from Cen X-4 but not from A0620-00.

Consider now the quiescent state, which is most relevant to the results reported here. We list three differences: (1) The X-ray luminosity of Cen X-4 is  $(3-10) \times 10^{32} \text{ ergs s}^{-1}$  ( $d = 1.2 \text{ kpc}$ ), whereas no X-rays at all are detected from A0620-00,  $L_x < 10^{32} \text{ ergs s}^{-1}$  ( $d = 1.0 \text{ kpc}$ ). (2) The emission line spectrum of Cen X-4 includes high-excitation lines (e.g., He II  $\lambda 4686$ ) and Balmer lines, whereas only Balmer lines are present in the spectrum of A0620-00. (3) Chevalier *et al.* (1989) found that the minimum in Cen X-4's light curve near spectroscopic phase 0.25 has a complex and variable shape (see § IVb); in contrast, the corresponding portion of A0620-00's light curve has a regular shape and is relatively stable.

Some of the above optical differences may be due to the very different boundary conditions at the inner edge of the accretion disk. In Cen X-4 the disk must either terminate at a magnetosphere or at the hard surface of the neutron star. The observed X-ray flux may be produced at this boundary layer (e.g., Patterson and Raymond 1985). Furthermore, much of this X-ray/UV flux may be intercepted by the secondary and the outer disk if the boundary layer region is puffed-up out of the disk plane. If so, this could account for the high-excitation emission lines and some of the anomalies in the light curve. In the case of A0620-00, on the other hand, no comparable boundary-layer emission is expected if its surface is the "no return" event horizon of a black hole. In particular, no X-rays ( $E \gtrsim 1 \text{ keV}$ ) are expected (de Kool 1988) or observed. Moreover, very little of the UV radiation from the planar surface of the inner disk would be intercepted by the outer disk and the secondary (compared to the radiation emitted by a boundary layer that protrudes far out of the disk plane). This picture may explain why the primary minimum in A0620-00's light curve is deep and relatively stable and why there is an absence of high-excitation emission lines in the optical spectrum.

Shortly before his untimely death, Yoram Avni kindly made available to us his light curve analysis program, which plays a



crucial part in the work reported here; equally important in recent years were Yoram's incisive and insightful comments on our dynamical studies of A0620-00 and Cen X-4. We are grateful to R. Martello for help in reducing the photometric data, D. Latham for measuring the radial velocity of HD 131719, and several CTIO staff members, especially S.

Heathcotte, for help with the observations. We also thank several people for useful discussions and comments on the manuscript, including R. Belian, K. Horne, S. Rappaport, J. Raymond, and E. Schlegel, and we thank K. Modestino for her skillful preparation of the manuscript.

## REFERENCES

- Abt, H. A., Meinel, A. B., Morgan, W. W., and Tapscott, J. W. 1968, *An Atlas of Low-Dispersion Grating Stellar Spectra*.
- Al-Naimy, H. M. 1978, *Ap. Space Sci.*, **53**, 181.
- Avni, Y. 1978, in *Physics and Astrophysics of Neutron Stars and Black Holes*, ed. R. Giacconi and R. Ruffini (Amsterdam: North-Holland), p. 43.
- Belian, R. D., Conner, J. P., and Evans, W. D. 1972, *Ap. J. (Letters)*, **171**, L87.
- Blair, W. P., Raymond, J. C., Dupree, A. K., Wu, C.-C., Holm, A. V., and Swank, J. H. 1984, *Ap. J.*, **278**, 270.
- Bochkarev, N. G., Karitskaya, E. A., and Shakura, N. I. 1979, *Soviet Astr.*, **23**, 8.
- Bouvier, J., and Bertout, C. 1988, *Astr. Ap.*, **211**, 99.
- Canizares, C. R., McClintock, J. E., and Grindlay, J. E. 1980, *Ap. J. (Letters)*, **236**, L55.
- Chevalier, C., Illovaicky, S. A., van Paradijs, J., Pedersen, H., and van der Klis, M. 1989, *Astr. Ap.*, **210**, 114.
- Conner, J. P., Evans, W. D., and Belian, R. D. 1969, *Ap. J. (Letters)*, **157**, L157.
- Cowley, A. P., Hutchings, J. P., Schmidtke, P. C., Hartwick, F. D. A., Crampton, D., and Thompson, I. B. 1988, *A.J.*, **95**, 1231.
- de Kool, M. 1988, *Ap. J.*, **334**, 336.
- Evans, W. D., Belian, R. D., and Conner, J. P. 1973, in *Proc. on Transient Cosmic Gamma- and X-ray Sources*, ed. I. B. Strong (Los Alamos: Los Alamos National Lab.), p. 107.
- Gilliland, R. L., and Kemper, E. 1980, *Ap. J.*, **236**, 854.
- Horne, K., and Marsh, T. R. 1986, in *The Physics of Accretion onto Compact Objects: Lecture Notes in Physics*, Vol. 266, ed. K. O. Mason, M. G. Watson, and N. E. White (Berlin: Springer-Verlag), p. 1.
- Jacoby, G. H., Hunter, D. A., and Christian, C. 1984, *Ap. J. Suppl.*, **56**, 257.
- Kaluzienski, L. J., Holt, S. S., and Swank, J. H. 1980, *Ap. J.*, **241**, 779.
- Kazanas, D. 1986, *Astr. Ap.*, **166**, L19.
- Keenan, P. C., and McNeil, R. C. 1976, *An Atlas of Spectra of the Cooler Stars* (Columbus: Ohio State University Press).
- Landolt, A. U. 1983, *A.J.*, **88**, 439.
- Latham, D. W. 1988, private communication.
- Lucy, L. B. 1967, *Zs. Ap.*, **65**, 89.
- Matsuoka, M., et al. 1980, *Ap. J. (Letters)*, **240**, L137.
- McClintock, J. E., Petro, L. D., Remillard, R. A., and Ricker, G. R. 1983, *Ap. J. (Letters)*, **266**, L27.
- McClintock, J. E., and Remillard, R. A. 1986, *Ap. J.*, **308**, 110.
- Paczynski, B. 1971, *Ann. Rev. Astr. Ap.*, **9**, 183.
- Patterson, J., and Raymond, J. C. 1985a, *Ap. J.*, **292**, 535.
- . 1985b, *Ap. J.*, **292**, 550.
- Popper, D. M. 1980, *Ann. Rev. Astr. Ap.*, **18**, 115.
- Pylser, E., and Savonije, G. J. 1988, *Astr. Ap.*, **191**, 57.
- Robinson, E. L. 1976, *Ann. Rev. Astr. Ap.*, **14**, 119.
- Russell, H. N. 1945, *Ap. J.*, **102**, 1.
- Stauffer, J. R., Dorren, J. D., and Africano, J. L. 1986, *A.J.*, **91**, 1443.
- Tonry, J., and Davis, M. 1979, *A.J.*, **84**, 1511.
- van Paradijs, J., Verbunt, F., Shafer, R. A., and Arnaud, K. A. 1987, *Astr. Ap.*, **182**, 47.
- van Paradijs, J., Verbunt, F., van der Linden, T., Pedersen, H., and Wamsteker, W. 1980, *Ap. J. (Letters)*, **241**, L161.
- Vogt, S. S. 1975, *Ap. J.*, **199**, 418.
- Vrba, F. J., Herbst, W., and Booth, J. F. 1988, *A.J.*, **96**, 1032.
- Webbink, R. F., Rappaport, S., and Savonije, G. J. 1983, *Ap. J.*, **270**, 678.
- White, N. E., Fabian, A. C., and Mushotzky, R. F. 1984, *Astr. Ap.*, **133**, L9.
- White, N. E., and Marshall, F. E. 1984, *Ap. J.*, **281**, 354.
- Zahn, J.-P. 1977, *Astr. Ap.*, **57**, 383.

JEFFREY E. McCLINTOCK: Harvard-Smithsonian Center for Astrophysics, 60 Garden Street, Cambridge, MA 02138

RONALD A. REMILLARD: Massachusetts Institute of Technology, Center for Space Research, Room 37-595, Cambridge, MA 02139